Curvature Attributes and their Application to 3D Interpreted Horizons

Andy Roberts

Enterprise Oil Norge Ltd., Løkkeveien 103, P.O. Box 399, N-4001 Stavanger, Norway

Introduction

The advent of the interpretation workstation has allowed the generation and analysis of horizon attributes to develop rapidly. These days it is common to find that a press of a button can produce over forty attributes. However, the skill is not in their production, but in their interpretation and integration with the rest of the data being analysed. Many attributes are introduced before their application is fully understood and commonly new attributes are just a minor modification of an existing one. So, why introduce yet more attributes? The reason is that curvature attributes are not new attributes at all, but already have a proven track-record in many other industries and disciplines outside of the oil industry e.g. medical brain scanners (Joshi *et al.* 1995), Optometry (Daniel & Barsky 1997) and Terrain Analysis (Wood 1996). This paper gives a brief insight into these curvature attributes and discusses some of their applications. From the infinite number of possible curvature attributes, only a small subset is presented, which are found most applicable to seismic data. It is surprising that curvature analysis has found only limited use within the oil industry, as the technique enhances aspects of mapped surfaces which are not readily obtained from the attributes in common use today. A full suite of formulae have been included in the paper, to allow easy implementation of the method on any workstation, which will hopefully encourage the more wide spread use and acceptance of the method.

Fig.1 explains curvature attributes in relation to the many other *surface-related* attributes. The purpose of a *surface-related* attribute is to enhance or bring out a particular aspect or property of a surface, which may otherwise be difficult or impossible to observe, without introducing artefacts. The term *surface* is taken to mean any surface, which is either flat, interpreted or used to control a window from which a volume attribute can be extracted. *Surface-related* attributes can be grouped into three main categories. *Surface-associated* attributes are those which use a surface to extract values from a secondary data source e.g. seismic amplitude, coherency cube, complex trace and AVO data. *Surface-derived* attributes are computed directly from the surface itself. The most common attributes in this category are the first derivative type, which include the *dip*, *edge* and *azimuth* attributes as well as other map derived attributes such as isochore, trend and residual maps (Brown 1996, Chapter 8). Within this category, curvature falls into a separate group called second derivative attributes, which also includes Laplace-based methods. Both *surface-associated* and *surface-derived* attributes can be plotted directly to the screen or a plotter. The third category is called *surface-rendered* attributes. Rather than the conventional map view, a surface can be portrayed in three-dimensions using 3D visualisation and illumination techniques (Brown 1996, Chapter 8). These types of displays can be very effective in identifying faults and other subtle map features, but can require extensive image manipulation in order to extract the full benefit. It is also possible to pass the other two attributes classes through this rendering process, as indicated by the dotted lines on Fig.1.

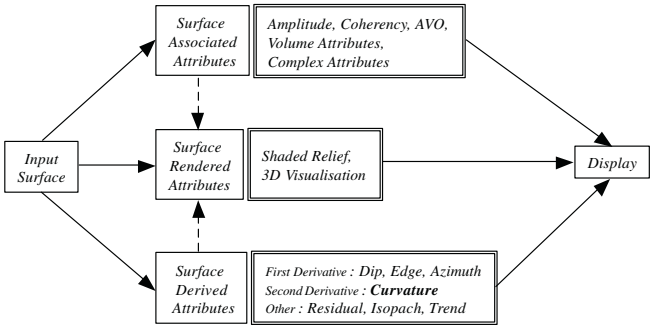

Fig.1 Classification of surface-related attributes. Surface-related attributes fall into three main categories : *surface-associated*, *surface-rendered* and *surface-derived*.

What is curvature ?

Curvature is a two-dimensional property of a curve and describes how bent a curve is at a particular point on the curve i.e. how much the curve deviates from a straight line at this point. For a particular point on a curve, its curvature is defined as the rate of change of direction of a curve. If we consider a point **P** on a curve (Fig.2), then the curvature at this point is defined as the rate of change of angle $d\omega$ with respect to the arc length dS. There also exists a circle, having a common tangent T at point **P**, which makes the greatest possible contact with the curve. This circle is called the *osculating circle*. The radius of this circle is defined as the *radius of curvature, R*. A circle is of course bent by the same amount all away around its circumference and therefore has constant curvature, K. We can use this particular property of a circle to derive the curvature relationship:

$$K = \frac{d\omega}{dS} = \frac{2\pi}{2\pi R} = \frac{1}{R} \qquad (1)$$

Curvature is simply the reciprocal of the *radius of curvature*. From this simple relationship we can see that the smaller the *radius of curvature*, the more bent the curve is and hence the larger the curvature. If we consider the limiting case where the *radius of curvature* is infinite, then locally the circle would approximate to a straight line and hence have zero curvature. The curvature can also be expressed in terms of derivatives (see Thomas, 1972, 473-475):

$$K = \frac{d^2y/dx^2}{\left(1 + (dy/dx)^2\right)^{3/2}} \qquad (2)$$

Examination of this relationship reveals that curvature is closely related to the second derivative of a curve. Often the second derivative is used as a direct measure of curvature,

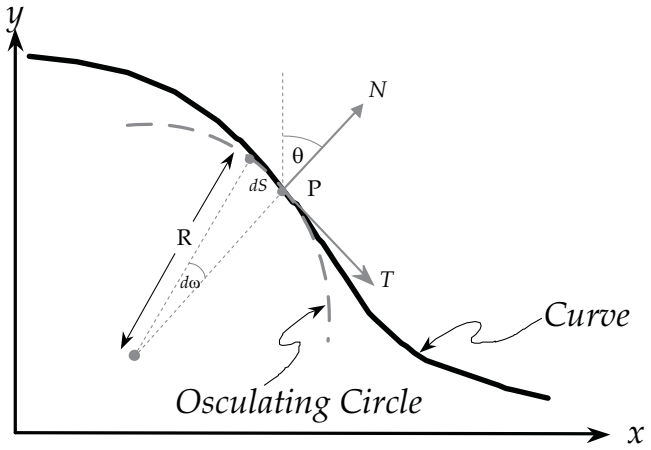

Fig.2 Mathematical definition of curvature. For a particular point **P** on a curve, the curvature can be defined in terms of the *radius of curvature, R* of the osculating circle. This circle possesses a common tangent *T* with the curve. *N* is the vector normal to the curve at point **P**, which defines the local dip angle θ. The curvature at point **P** is defined as the reciprocal of the *radius of curvature*. See text for more details.

however it is only in the special case of zero dip that this assumption is strictly valid. However, for small dip values it makes a close approximation.

Another way to visualise curvature is to consider a 2D cross-section through a particular mapped surface, as is displayed in Fig.3. In this figure the vectors, which are normal to the surface, are drawn in grey at regular intervals along the horizon. Where the horizon is either flat or planar dipping, the corresponding vectors are all parallel and thus the horizon has zero curvature at these locations. Where the horizon forms an anticline or ridge feature, the vectors all diverge and the curvature is defined as positive. Where the curve forms a syncline, the vectors all converge and the resulting curvature is defined as negative. This figure defines the curvature sign convention used in this paper. Different oriented cross-sections through the same point on the surface result in different curvatures. It is this potential variability in curvature, depending on the orientation of the cross-section, which necessitates an explicit definition of curvature for three-dimensional surfaces.

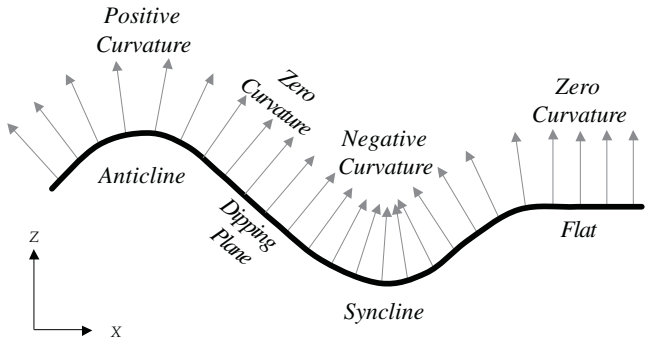

Fig.3 Sign convention for curvature attributes. The grey arrows represent vectors, which are normal to the surface. Where these vectors are parallel on flat or planar dipping surfaces, the curvature is zero. Where the vectors diverge over anticlines, the curvature is defined as positive and where they converge over synclines, the curvature is defined as negative.

The two-dimensional concept of curvature can be easily extended into three-dimensions (Fig.4). A curve can be constructed by mathematically cutting the surface with a plane. The intersection the plane makes with the surface describes a curve from which the curvature can be calculated at any point along the curve. To help visualise this, consider the surface as the skin of an apple and the mathematical plane as a knife. The cut made by the knife into the skin of the apple represents the curve. Cutting the apple through the middle creates a circle, with its corresponding curvature. However, cutting the top off the apple results in a much smaller circle and hence larger curvature. There are of course an infinite number of cuts which can be made and hence an infinite number of curvatures which can be extracted. It is found that the most useful subset of curvatures are those defined by planes which are orthogonal to the surface and these are called *normal curvatures*. It is this type which form the bulk of the curvature attributes described in this paper.

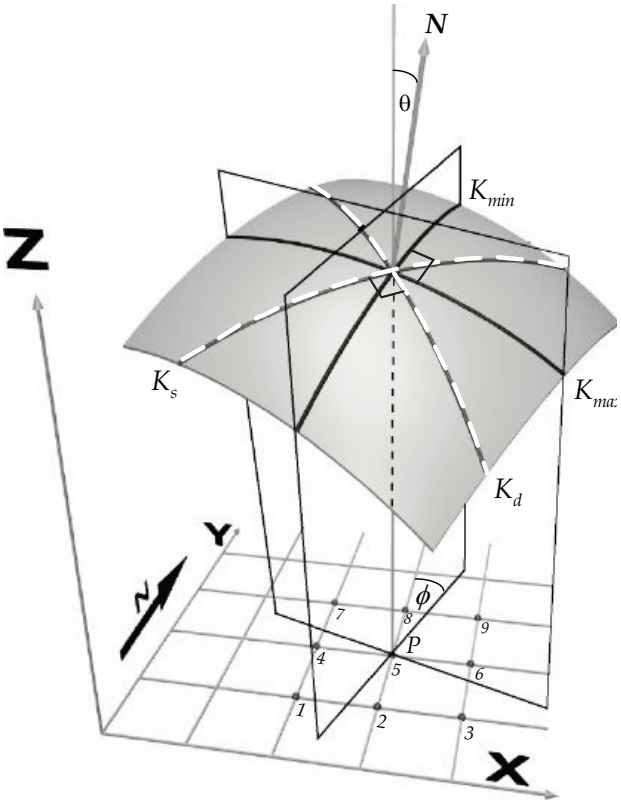

Fig.4 Curvature in three-dimensions. x and y represent the map axes, with z representing the time or depth axis. Note the intersection of two orthogonal planes with the surface, which describes the *maximum curvature*, K_{max} and the *minimum curvature*, K_{min}. Two other orthogonal *normal curvatures*, the *dip curvature*, K_d and the *strike curvature*, K_S are also drawn on the surface. See text for a more detailed description. *N* is the vector normal to the surface at point **P**, which makes an angle θ with the vertical, called the *dip angle*. The orientation of any *normal curvature* can also be extracted, with the angle ϕ being the *orientation of minimum curvature*. The location of the underlying gridded map surface has been added for reference, with the additional annotation of nine grid nodes. These represent the 3x3 grid cell used in the curvature calculation (Fig.9), where node 5 represents the point P whose curvature value is being calculated.

These *normal curvatures* can be combined in a number of different ways, which define important curvature properties relating to all surfaces. Firstly, the average of any two orthogonal *normal curvatures* through a point on a surface is constant and is defined as the *mean curvature,* K_m:

$$K_m = \frac{K_1 + K_2}{2} = \frac{K_{max} + K_{min}}{2} \qquad (3)$$

where K_1 and K_2 represent any pair of orthogonal *normal curvatures.* Secondly, from the infinite number of *normal curvatures*, which pass through a particular point on a surface, there exists one curve, which defines the largest absolute curvature. This is called the *maximum curvature* K_{max}. The curve perpendicular to K_{max} is called the *minimum curvature*, K_{min}. These two surface attributes are called the *principal curvatures*. They represent the extremes of *normal curvatures* and are best explained in terms of Euler's curvature formula (Rektorys 1969):

$$K_i = K_{max} \cos^2 \delta + K_{min} \sin^2 \delta \qquad (4)$$

where δ is the angle between the plane of a particular *normal curvature*, K_i and the plane of the *maximum curvature*, K_{max}. Eqn.4 states that any *normal curvature,* K_i at a point on a surface can be derived from the *principal curvatures*. A graphical representation of Eqn. 4 is illustrated in Fig.5, where the full set of *normal curvatures* have been calculated for five differently shaped surfaces. It is this combination of orthogonal curvatures which tells us something about the local shape of the surface.

Gaussian curvature describes a third important property relating to the bending of a surface. It is defined by the product of the *principal curvatures*:

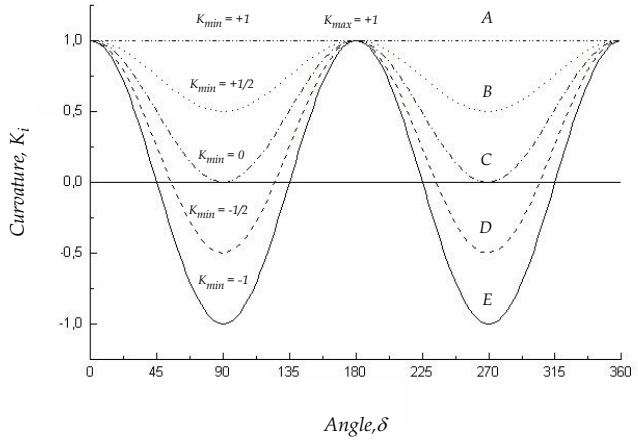

Fig.5 Graphical representation of Euler's curvature formula **(**Eqn.4). The *normal curvature* for all orientations is defined here for five differently shaped surfaces: A = Spherical dome; B = Elongated dome; C = Cylindrical ridge; D = Elongated saddle; E = Perfect saddle. All the surfaces in this diagram have an identical K_{max} of +1, with K_{min} varying between ±1. Note for a particular surface how the curvature is repeated every 180° and the average of any two curvatures, which are 90° apart, is constant. This constant is defined as the *mean curvature*, K_m. The sphere is a special case where the *minimum curvature* and *maximum curvature* are equal and the same at all orientations.

$$K_g = K_{min} K_{max} \qquad (5)$$

This type of curvature, sometimes referred to as the *total curvature*, is named after Gauss and his Theorema Egregium (Gauss 1827), which means the wonderful theory. The theorem states that the isometric bending of a surface does not change the *Gaussian curvature* of points on that surface. In other words, if a surface is folded in some way, provided the surface is not broken, stretched or squeezed, then the *Gaussian curvature* remains constant. If we take a piece of paper and roll in into a cylinder or cone, then this operation does not alter the *Gaussian curvature*, as it remains unchanged and is always zero. A surface of this type is referred to as a *developable surface*. A flat surface has zero curvature in all directions, a cone has zero curvature in the *minimum curvature* direction and a non-zero curvature in the *maximum curvature* direction. Forming a cone or cylinder with a piece of paper only alters the *maximum curvature*, as the *minimum curvature* remains zero. Therefore, many shapes cannot be differentiated by *Gaussian curvature* alone, but require the addition of the *mean curvature* information. The detection of local shape from this combination of curvatures is summarised in Fig.6.

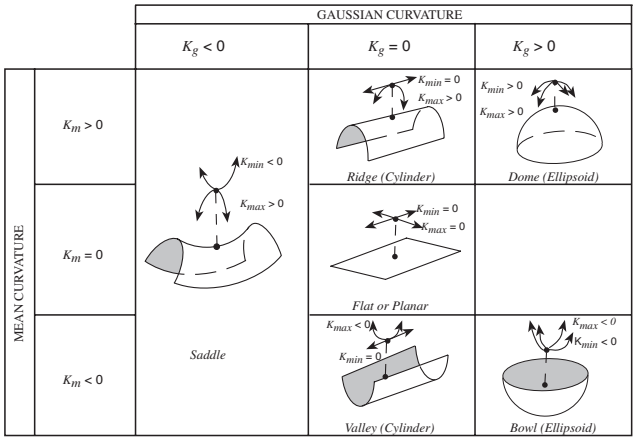

Fig.6 Curvature shape classification. Combination of *mean curvature* and *Gaussian curvature* allows the local shape of a surface to be described.

A brief history of curvature

Curvature has only recently been exploited to its full potential, due mainly to the advent of computers. However, being intimately related to geometry, the history and development of curvature goes back a long way. It probably all began in the third century BC, when Apollonius of Perga applied simple methods to find the radius of curvature, which were similar to those used by Huygens and Newton some two thousand years later. It wasn't until the fourteenth century that the next advances were made. Oresme (who is accredited with the invention of the graph) described two curves having a common tangent at a point. The inner most curve is the one with the greater curvature. He also noted that the curvature of a circle is constant and is equal to the inverse of its radius (Eqn.1). In the seventeenth century, Fermat, Descartes and Huygens made small additional contributions. What these scientists lacked was calculus, which was added by Newton and Leibnitz a few years later. Using calculus, Newton was able to describe the radius of curvature in terms of derivatives (Eqn.2). It was in fact Leibnitz who came up with the name *osculating circle*, but his work was not given much recognition as he unfortunately made a fundamental error. In the eighteenth

century, Euler developed much more mathematically rigorous methods to describe curvature e.g. Eqn.4, bringing the understanding a further step forward. The nineteenth century brought a significant contribution to curvature, when Gauss published his work on the theory of surfaces (Gauss 1827). Building on Euler's work, he realised that the total curvature of a particular point on the surface can be expressed as the product of the smallest and largest curvatures which pass through the point (Eqn.5). Since then, the contributions have mainly come in developing computer algorithms and finding useful applications. It is both interesting and humbling to note that some of the curvature related finite difference methods, which are now used in computer programs, were in fact developed in the early part of the last century (Marcus 1932; Nielsen 1920).

Curvature attributes and their application

Preparation and presentation

Before calculating curvature or in fact most other map attributes, it is worth mentioning the two P's: Preparation and presentation. As curvature is closely related to the second derivative of the surface, its quality is very susceptible to the level of noise contamination. There are often many sources for this noise on a mapped surface, e.g. geological, processing, acquisition and the horizon autotracking process. It is therefore recommended to prepare the surface before the curvature is computed, by applying some form of mild two-dimensional spatial filter. This filtering can be performed in many different ways, for example, iterative median filtering (Gallagher & Wise 1981) and weighted average filtering, where the weights can be distance related or a Gaussian type. It is often necessary to apply multiple iterations of the same filter before a satisfactory result is obtained. All have the effect of a high-cut filter and attenuate the very rapid changes on the surface, most of which are probably due to noise contamination. Leaving high frequency noise in a surface can result in the real curvature being obscured. Filtering is often a compromise between trying to remove the noise effectively, without reducing the resolution and obscuring too much of the detail. This form of surface conditioning is a very important aspect of the curvature calculation process. Time invested in appropriate filtering of the surface will result in a much more satisfactory result.

The second important point is presentation. All too often a particular attributes effectiveness is diminished by the use of an inappropriate colour scheme. Careful selection of the colour map for display on the screen can often make a tremendous difference to what the eye can see. Choice of colours is a very personal thing, given the prevalence of colour-blindness and individual colour sensitivity. What one person may see may be almost invisible to the next. It is therefore worth investing a good deal of time in designing tailor-made colour tables for a particular attribute display.

Scale of investigation

The mathematical definition of curvature for a continuous surface is explicit. However, most mapped surfaces are in a gridded form and introduce the complication of how the surface is sampled. This brings in the concept of the scale of investigation. In extracting curvature information from a surface, the sampling interval and hence aperture size must be defined. It is best described by the use of an analogy. Imagine a large mound of stones 100m across and 10m high. From a distance, this mound would look like a smooth hill i.e. a surface with small curvature. At a position on or close to the mound, the individual stones can be resolved, indicating that the mound is a very rough surface, with a correspondingly high local curvature. If each individual stone is examined, some may be rough, some rounded and some flat i.e. all have quite different curvature values. Calculating the curvature of the mound of stones therefore depends on the scale at which measurements are taken. The sampling criteria used must therefore be consistent with the type of information being extracted i.e. large apertures for regional trends (long wavelength structures) and small apertures for local surface detail (short wavelength structures). The effective aperture size can be varied in a number of different ways. One method is to alter the number of grid nodes used in the curvature calculation. However, using too many grid nodes increasing the complexity of the calculation, which impacts the speed of computation. A simpler method is to increase the aperture size of filters used in the pre-processing and/or decimating the horizon grid in some manner i.e. using every n^{th} line and n^{th} trace. See Stewart & Podolski (1998) for a more detailed description of this issue.

Data set description

The data set used in this study is a small subset of a large 3D survey, which is located in the North Sea. This subset volume is approximately 6km x 8km (300 lines x 350 traces) and was acquired in an east-west direction. The mapped surface displayed in was created in a two step process. Firstly, every 20^{th} line and 20^{th} trace was interpreted, with the remaining areas being infilled by a horizon autotracker. Secondly, the surface was filtered by a 3x3 iterative median filter, followed by a 5x5 distance-weighted average filter. All the curvature attributes presented in this paper are based on this filtered two-way-time surface shown in Fig.7. It is assumed that the time scale is interchangeable with depth. Examination of the seismic section A-B (Fig.8) indicates that the data is generally of good quality and continuity, with the mapped surface varying in time from 3650ms to 3950ms. Structural highs and lows, as well as a number of large and small faults punctuate the surface, although some of these faults are difficult to see on both the seismic section and the map display.

Computing curvature

There are many different ways the curvature of a gridded surface can be calculated, some of which are summarised in Stewart & Podolski (1998) and compared in Flynn & Jain (1989). As mapped surfaces created on interpretation workstations are in a gridded form, they are ideally suited for curvature calculation. The method used in this paper uses a least squares quadratic approximation to the mapped surface (Young 1978; Evans 1979; Wood 1996). In order to calculate the curvature at a particular point, a local quadratic surface (Eqn.6) is fitted in a least squares sense by using the surrounding eight grid values (Fig.9). Using this 3x3 grid cell approach, the calculation of the coefficients in Eqn.6 reduce to a series of simple arithmetic expressions
(Eqns. 7 to12):

$$y = ax^2 + by^2 + cxy + dx + ey + f \qquad (6)$$

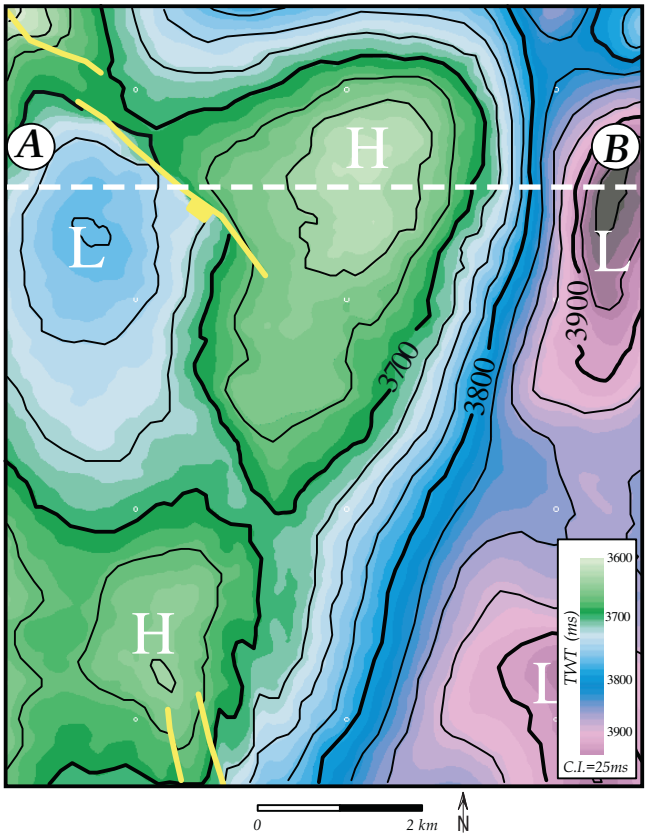

Fig.7 Time structure map. This surface forms the input to all the attributes presented in this paper.

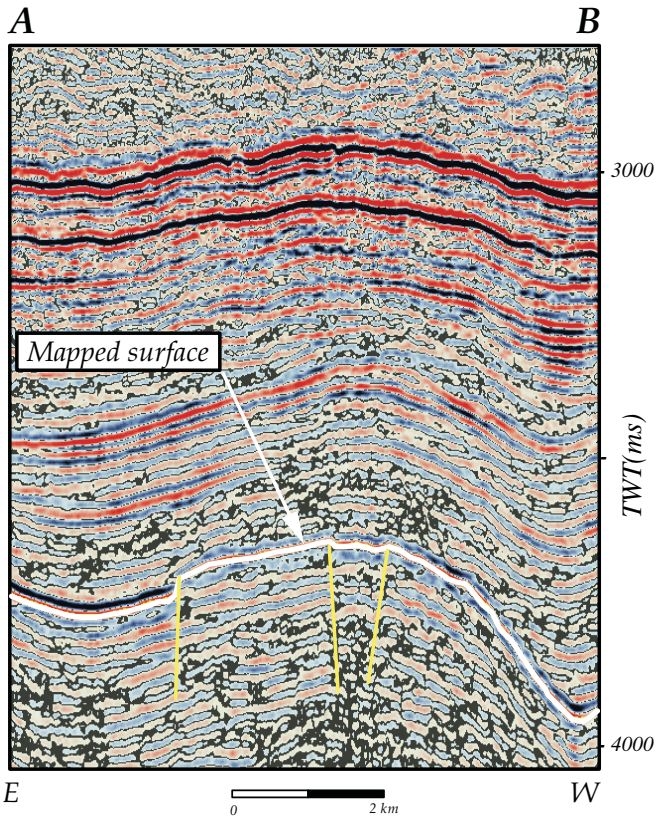

Fig.8 Seismic section A-B. For line location see Fig.7.

$$a = \frac{1}{2}\frac{\partial^2 z}{\partial x^2} = \frac{(Z_1 + Z_3 + Z_4 + Z_6 + Z_7 + Z_9)}{12\Delta x^2} - \frac{(Z_2 + Z_5 + Z_8)}{6\Delta x^2} \quad (7)$$

$$b = \frac{1}{2}\frac{\partial^2 z}{\partial y^2} = \frac{(Z_1 + Z_2 + Z_3 + Z_7 + Z_8 + Z_9)}{12\Delta x^2} - \frac{(Z_4 + Z_5 + Z_6)}{6\Delta x^2} \quad (8)$$

$$c = \frac{\partial^2 z}{\partial x \partial y} = \frac{(Z_3 + Z_7 - Z_1 - Z_9)}{4\Delta x^2} \quad (9)$$

$$d = \frac{\partial z}{\partial x} = \frac{(Z_3 + Z_6 + Z_9 - Z_1 - Z_4 - Z_7)}{6\Delta x} \quad (10)$$

$$e = \frac{\partial z}{\partial y} = \frac{(Z_1 + Z_2 + Z_3 - Z_7 - Z_8 - Z_9)}{6\Delta x} \quad (11)$$

$$f = \frac{2(Z_2 + Z_4 + Z_6 + Z_8) - (Z_1 + Z_3 + Z_7 + Z_9) + 5Z_5}{9} \quad (12)$$

where Z_1 to Z_9 refer to the surface grid node values as illustrated in Fig.9 and Δx is the distance between grid nodes. Larger grid cell sizes e.g. 5x5 can be used (Wood 1996), but these require solutions to a large set of normal equations. Keeping the number of grid cells small allows for the rapid computation of curvature, comparable to the speed of calculation of the *dip angle* and *azimuth* attributes. All the curvature attributes presented in this paper are based on this approach and are described in more detail below. The coefficients from Eqn.7 to 12 can also be used to derive the *dip angle* (Eqn.13) and *azimuth* (Eqn.14) attributes, which are plotted in Fig.10 and Fig.11 respectively. These figures have been included to allow comparison to the curvatureattributes. Both these attributes bring out some of the main lineaments contained within the surface.

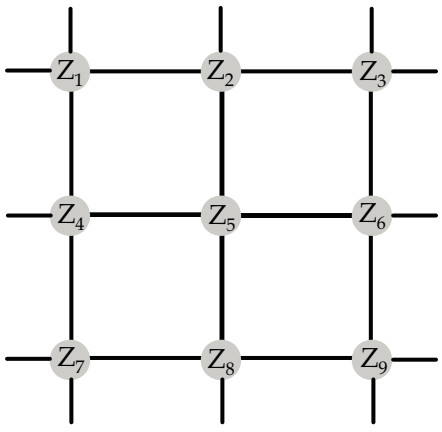

Fig.9 3x3 grid cell. This is the aperture size used in the computation of all the curvature, *dip angle* and *azimuth* attributes.

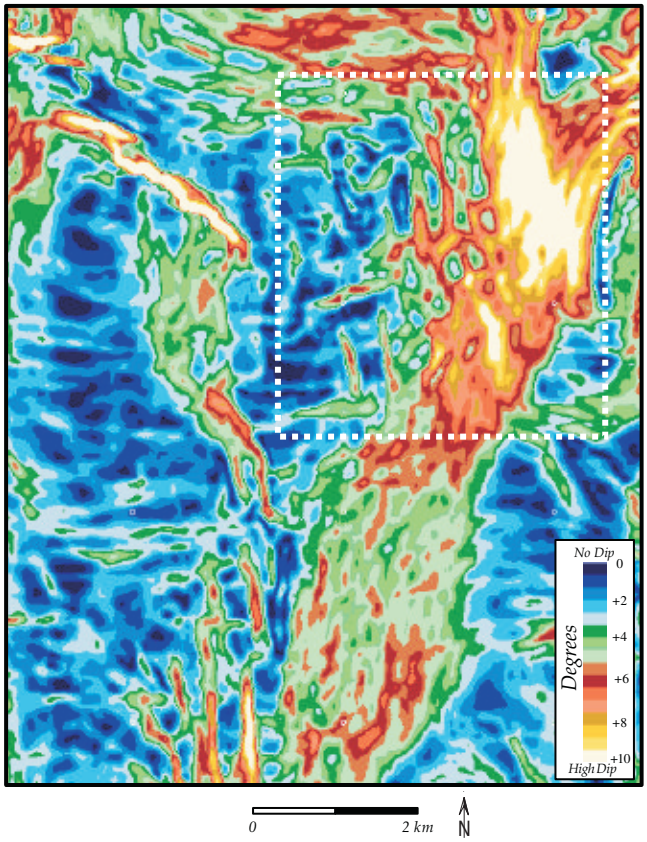

Fig.10 D*ip angle* attribute. This represents the angle of the maximum dip. The white dashed box represents the location of the enlarged display in Fig.25B.

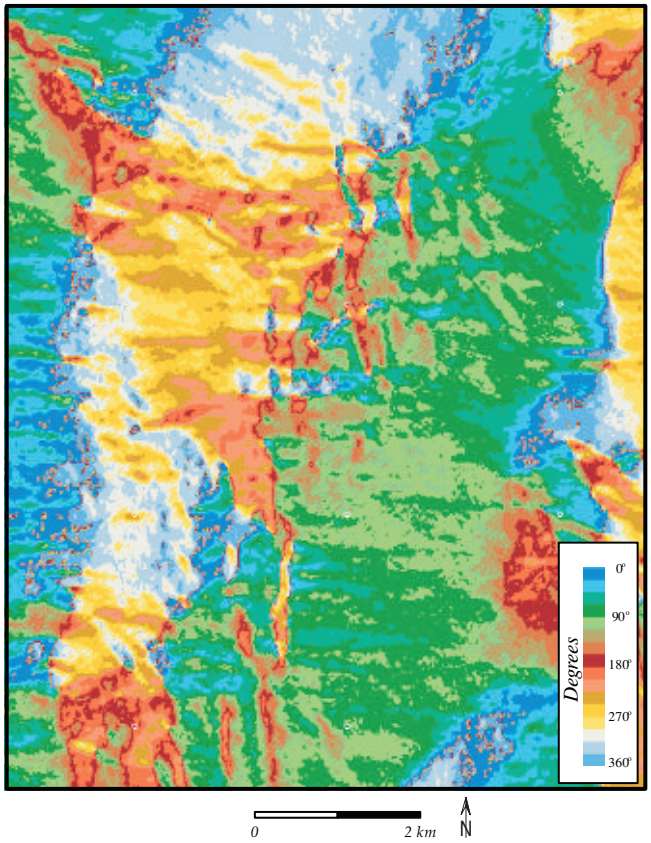

Fig.11 *Azimuth* attribute.

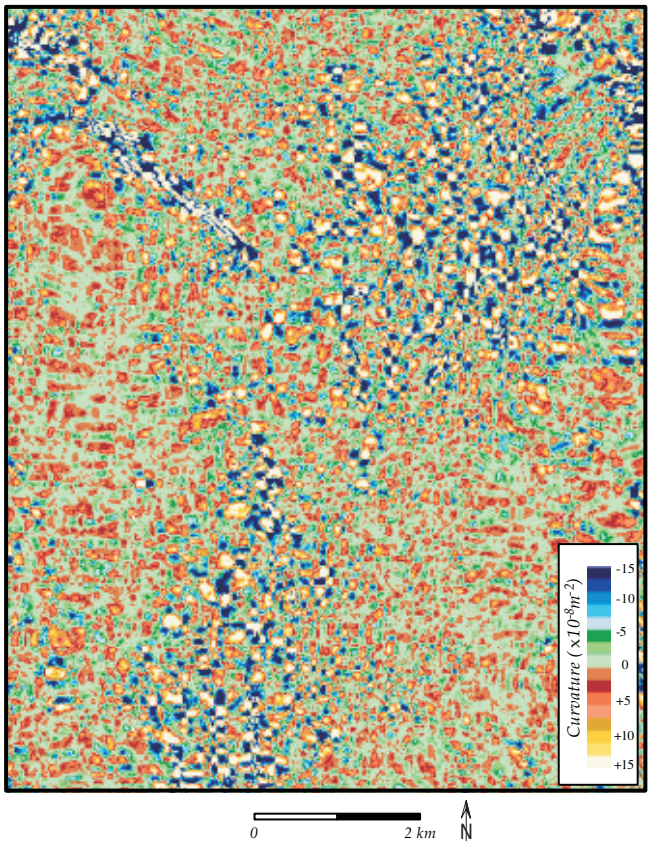

Fig.12 *Gaussian curvature, K*g.

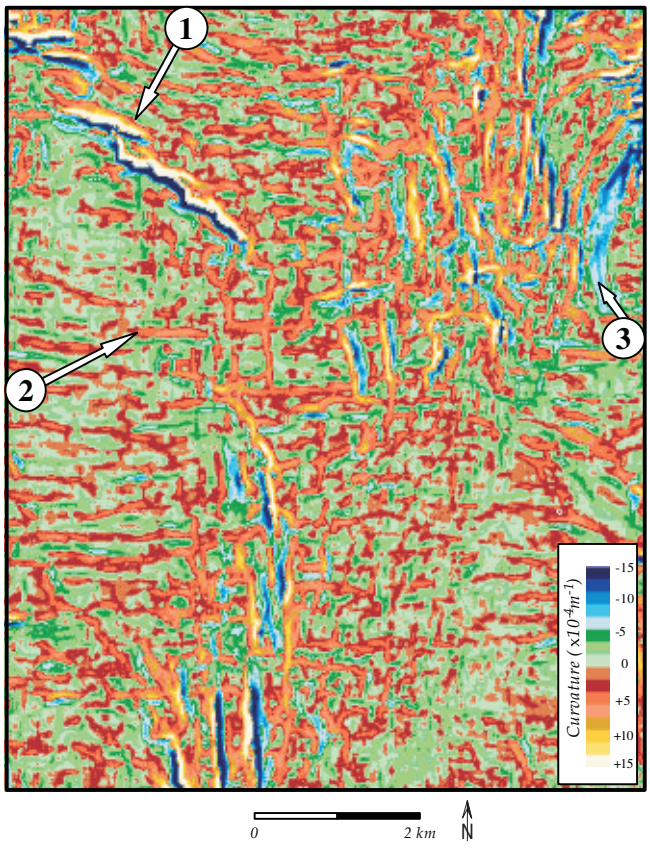

Fig.13 *Maximum curvature, K*max. See text for details.

Used in combination, these two attributes can be a useful aid to fault interpretation. Note the *dip angle* has been used in preference to the more common *dip* or *slope* attributes. This is because the *dip* attribute is potentially unconfined, whereas the *dip angle* is restricted between 0° and 90°, although visually the two attributes are almost identical.

$$Dip\ Angle = \tan^{-1}\left(\sqrt{d^2 + e^2}\right) \qquad (13)$$

$$Azimuth = \tan^{-1}\left(\frac{e}{d}\right) \qquad (14)$$

Mean Curvature, K_m

Although the *mean curvature* represents an important surface property (See Eqn.3), it is in itself not a particularly useful visual attribute. This is because it tends to be dominated by and consequently visually similar to the *maximum curvature*. However, the *mean curvature* is very important because it is used to derive many of the other curvature attributes and is defined as follows (Rektorys 1969):

$$K_m = \frac{a\left(1+e^2\right) - cde + b\left(1+d^2\right)}{\left(1+d^2+e^2\right)^{3/2}} \qquad (15)$$

Gaussian Curvature, K_g

Gaussian curvature is defined as the product of the *principal curvatures* (Eqn.5) and is displayed in Fig.12. It can be calculated using Eqn.16 (See Rektorys 1969).

$$K_g = \frac{4ab - c^2}{\left(1+d^2+e^2\right)^2} \qquad (16)$$

Both Lisle (1994) and Wen & Townsend (1997) have suggested *Gaussian curvature* as a method to delineate faults. A comparison between Fig.12 and Fig.10 clearly shows that *Gaussian curvature* is not a good attribute for this type of operation. It is generally observed that many seismic-based mapped surfaces have *minimum curvature* values which are small and fluctuate around zero. Consequently, *Gaussian curvature,* being a product of curvatures, often exhibits rapid sign changes. Computing the absolute *Gaussian curvature* can alleviate this problem. Although this attribute has mathematical and geometrical significance, it has only limited application to mapped surfaces, but again forms an important component in deriving the other curvature attributes.

Maximum Curvature, K_{max}

The *maximum curvature* of the surface is displayed in Fig.13. By combining Eqn.3 and Eqn.5 the following relationship for K_{max} can be derived (Peet & Sahota 1985):

$$K_{\max} = K_m + \sqrt{K_m^{\,2} - K_g} \qquad (17)$$

This curvature attribute is very effective at delimiting faults and fault geometries. A fault on this attribute is represented by the juxtaposition of positive curvature values (red/yellow) and negative curvature values (blue/green). Note the enechelon set of faults on the NW part of the map, indicated by 1) in Fig.13. In addition, the curvature also defines the orientation of these faults, as positive curvature values represent the upthrown side and the negative values the downthrown side of the fault.

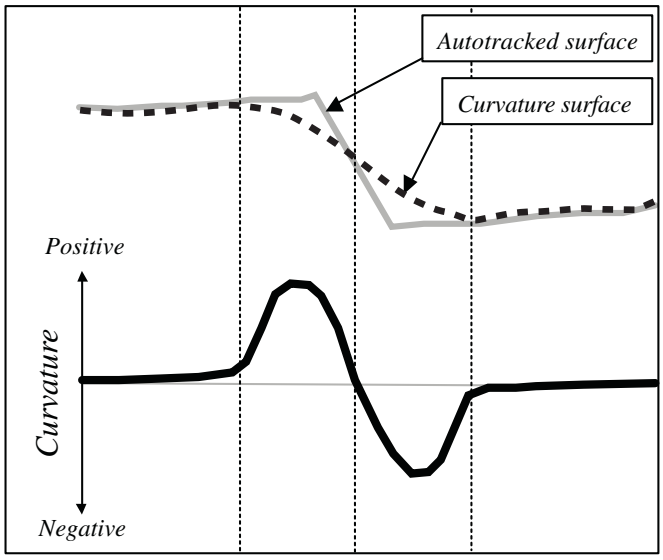

Fig.14 Fault delineation. Due to filtering and quadratic approximations, the surface used in the curvature calculation represents a smoothed version of the original surface. This has the effect of introducing anomalous curvature values over the fault, with high positive curvature on the upthrown side and high negative curvature on the downthrown side. Note that the zero crossing curvature point represents the centre of the fault plane.

Thus, these particular faults all downthrow to the SW. This fault delimiting property is in fact an artefact of the curvature calculation process, which is illustrated in Fig.14. The pre-filtering and least squares approximation have an effect of smoothing over the abrupt changes which are associated with the faulted surface. Essentially the curvature algorithm sees a smoothed version of the continuous surface, which was created by the autotracker. Although the input surface has almost zero curvature over the fault zone, the smoothed version introduces higher positive curvature values on the upthrown side and larger negative values on the downthrown side. It is this reversal in the curvature values which enables the direction of throw of the fault to be determined.

These faults are also seen on the *dip angle* map (Fig.10) as simple lineaments of higher angle. However, it is not possible to differentiate between a fault and a lineament, such as a ridge, with this type of first derivative based technique. Curvature has the advantage of containing shape information, allowing the faults to be differentiated from other surface lineaments. Lineaments, such as ridges and valleys, are represented by an isolated colour, examples of which are indicated by 2) and 3) respectively in Fig.13.

In addition to the orientation of faults, the magnitude of each fault is also described by the *maximum curvature*. This situation is illustrated in Fig.15, where the low K_{max} values have been greyed-out from the colour table. All that remains in the figure are the larger K_{max} values, which are associated with the larger faults and lineaments contained within the surface.

Minimum Curvature, $K_{\min}$

The *minimum curvature* of the surface is displayed in Fig.16 and is defined by Eqn.18:

$$K_{\min} = K_m - \sqrt{K_m^{\,2} - K_g} \qquad (18)$$

Comparisons between the scale bars in Fig.16 and Fig.13

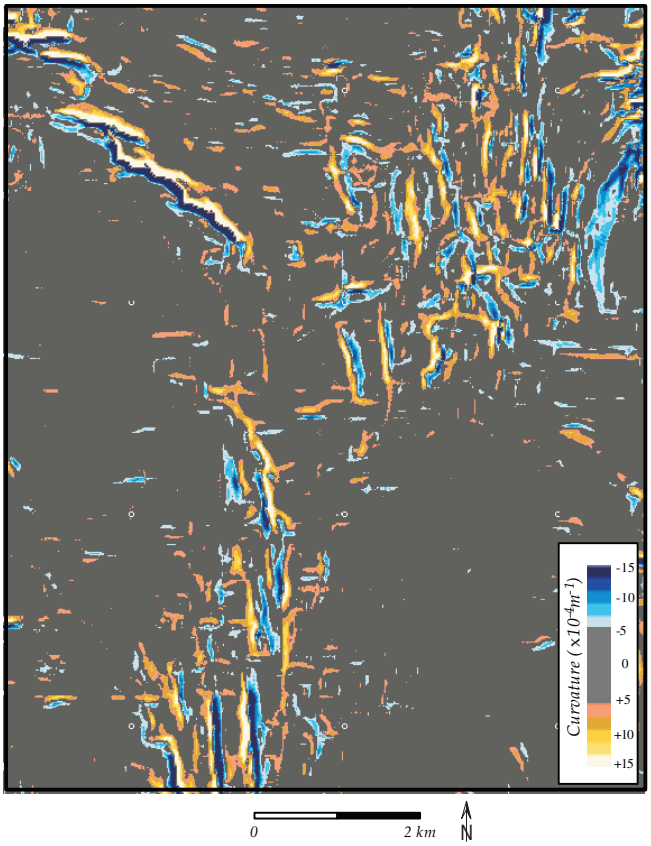

Fig.15 *Maximum curvature* with low curvature values greyed-out. Only the larger faults and surface lineaments are now visible.

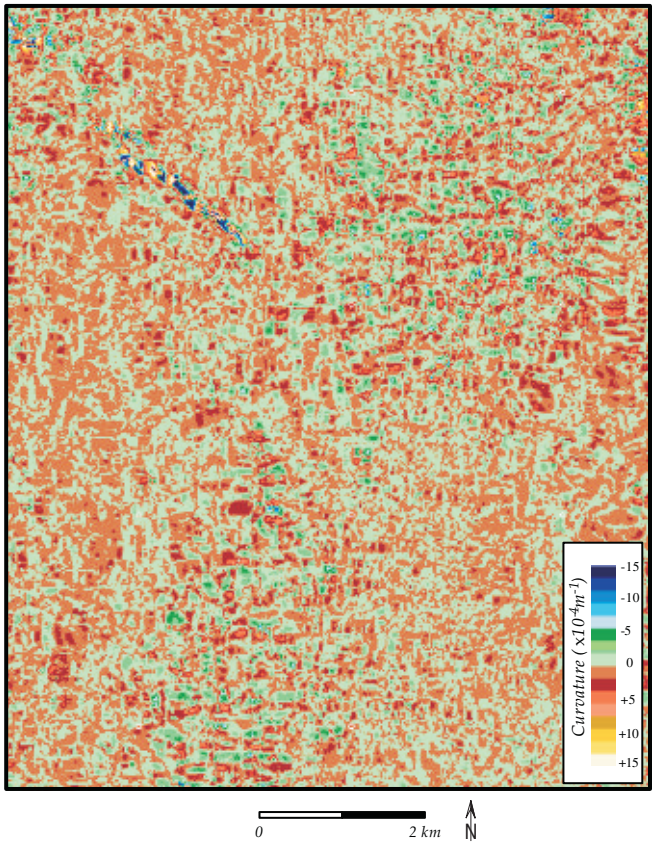

Fig.16 *Minimum curvature,* $K_{\min}$.

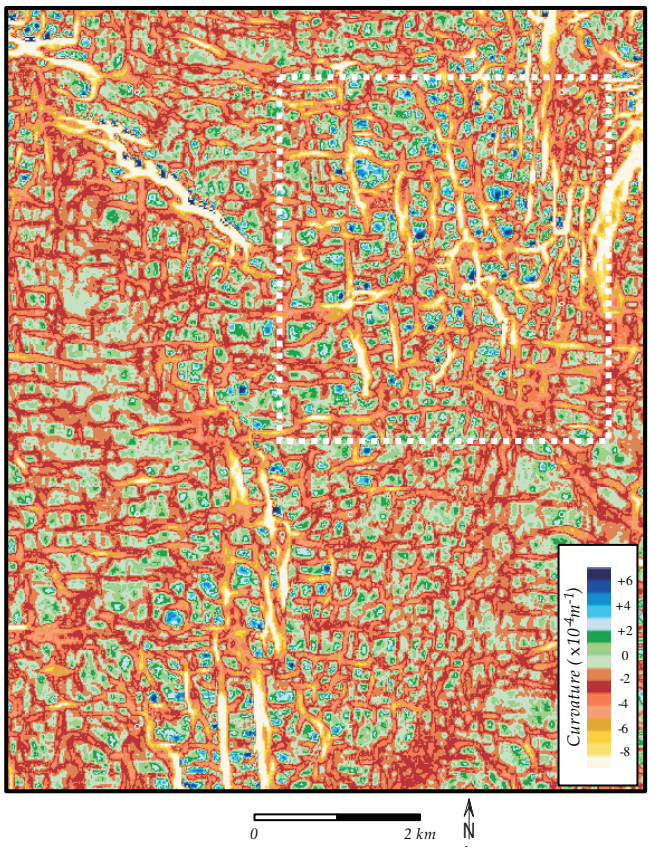

Fig.17 *Most negative curvature, K-*. The white dashed box represents the location of the enlarged display in Fig.25A.

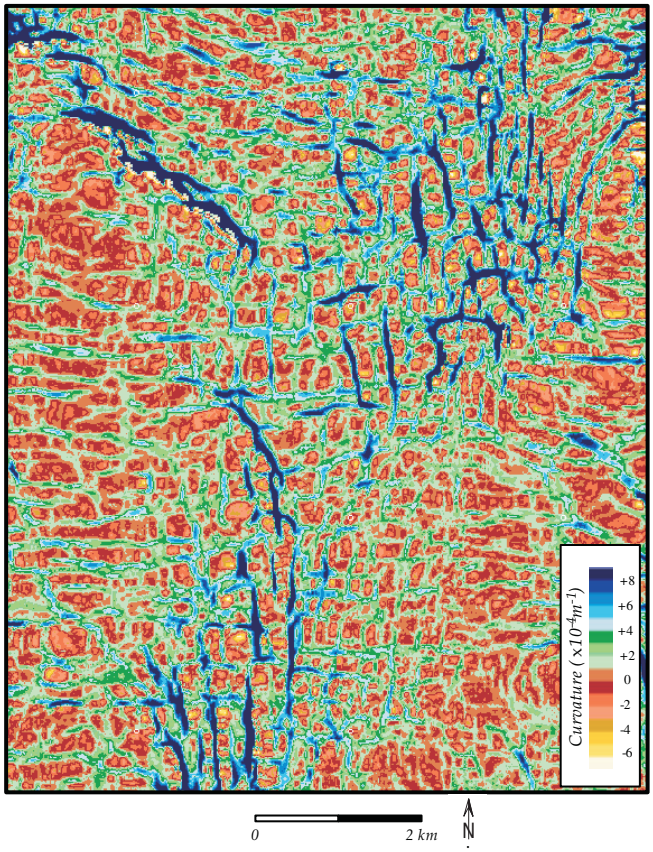

Fig.18 *Most positive curvature, K+*.

indicate that the K_{min} values are significantly smaller than the K_{max} values. When the K_{min} values are very small or zero, this indicates that the surface is a *developable surface*. Where K_{min} are large, this potentially indicates locations where non-isometric distortion of the surface has occurred i.e. where the surface is potentially faulted and fractured. Although visually this attribute can often appear noisy, it can sometimes be diagnostic in identifying fractured areas and is used to compute other curvature attributes.

Most Positive and Negative Curvatures, K_+ **and** K_-

The first derivative based attributes (*dip*, *edge* and *azimuth*) are used mainly to detect edges, which are associated with asymmetric (faults) and symmetric (ridges/valleys) surface features. The *maximum curvature* attribute (Fig.13) contains a great deal of information that can sometimes be confusing. An edge-type display can be derived by searching all possible *normal curvatures* for the most positive or most negative values. This can be readily obtained by setting the coefficients *d* (Eqn.10) and *e* (Eqn.11) to zero in Eqns.17 and 18 (Young 1978). The resulting attributes are called the *most positive curvature*, K_+ and the *most negative curvature*, K_-

$$K_+ = (a+b) + \sqrt{(a-b)^2 + c^2} \qquad (19)$$

$$K_- = (a+b) - \sqrt{(a-b)^2 + c^2} \qquad (20)$$

It is now possible to see almost every single lineament contained within the surface, with the faulting and lineaments taking on a polygonal appearance. The magnitude of the lineament is also preserved, allowing better lineament discrimination. However, the shape information is not preserved in this attribute, making it comparable to the first derivative methods (See attribute comparison discussion below). The east-west lineaments observed in Fig.17 and Fig.18 might be interpreted as an acquisition or processing footprint. However, this is a regional phenomena which is also observed on an overlapping 3D survey, located to the east, which was acquired at a different orientation. This type of attribute can be easily incorporated into a 3D visualisation display and this is illustrated in Fig.19. Incorporating the curvature in this way exaggerates both the fault and smaller linear features on the surface, making curvature a useful addition to this type of *surface-rendered* method.

Curvature and stress

Many authors have used curvature or curvature related attributes to predict fracture intensities over mapped structures (Lisle 1995; Murray 1968; Stewart & Podolski 1998). This correlation between curvature and fractures relates to the stresses experienced when a bed is folded or buckled. These induced stresses are illustrated in Fig.20, where anticlinal folding alters the bed length and induces stresses throughout the layer, with expansion increasing towards the top and compression increasing towards the base. The *neutral surface* is a special case where no stresses occur. This type of deformation can result in complex fault and fracture geometries (See Price & Cosgrove 1990 p. 378-383), caused by differential stresses and hydraulic fracturing. The stresses experienced at the top of the layer can be calculated using Eqn.21 (See Price & Cosgrove 1990, p. 190):

$$\text{Stress, } \sigma = \frac{h\,E}{2R} = \frac{h\,K\,E}{2} \qquad (21)$$

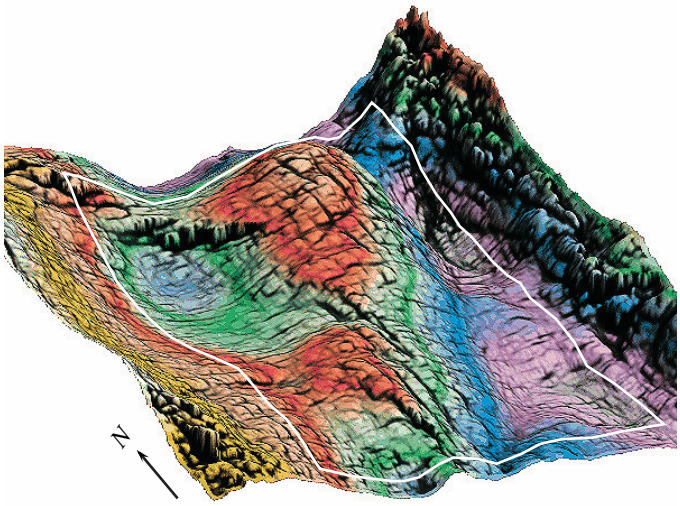

Fig.19 3D visualisation of curvature. The *most negative curvature* is incorporated as an intensity overlay on a 3D rendering of the time structure surface. This has the effect of exaggerating the faults and lineaments contained within the surface. Note the areal extent of this map is slightly larger than the time map displayed in Fig.7, whose extent is indicated by the white box. Structural highs are indicated by yellow/red and lows by blue/purple colours.

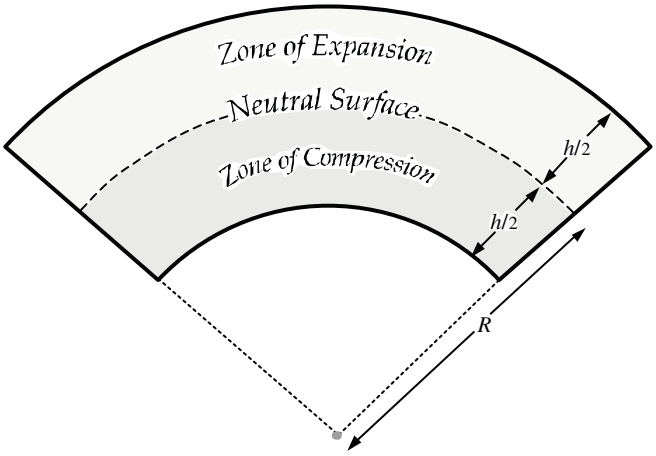

Fig.20 Curvature and stress. As a geological layer of thickness *h* is folded, the zone above the *neutral surface* experiences extension, as opposed to compression below this surface. The *neutral surface* is a surface which experiences no stress.

where *h* is the thickness of layer, *E* is the *Young's modulus* of the material and *R* the *radius of curvature* with a corresponding curvature, *K*. In three-dimensions, *K* would represent the *maximum curvature*. Eqn.21 states that for rocks having a similar *Young's modulus*, the stresses within a layer depend on the amount of curvature and the distance from the *neutral surface*. This type of layer or beam bending also represents an important area in engineering and the reader is referred to Timoshenko & Woinowsky-Krieger (1959) for a more detailed treatment.

Unfortunately, geological formations are not simple beams. The curvature of a mapped surface can be created by effects other than folding e.g. erosional unconformities and

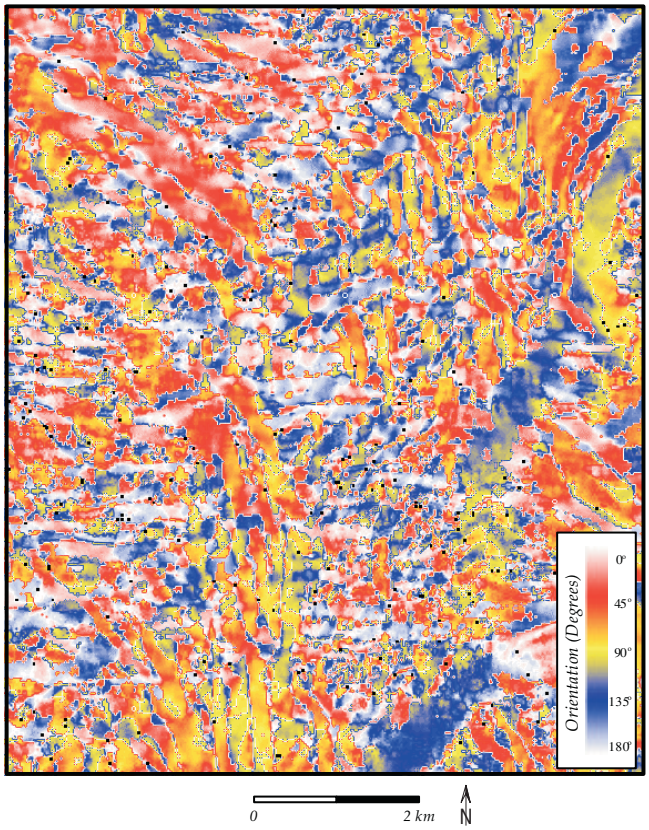

Fig.21 *Orientation of maximum curvature,* O_{max}. Note that the orientation angle is only defined between 0^o and 180^o.

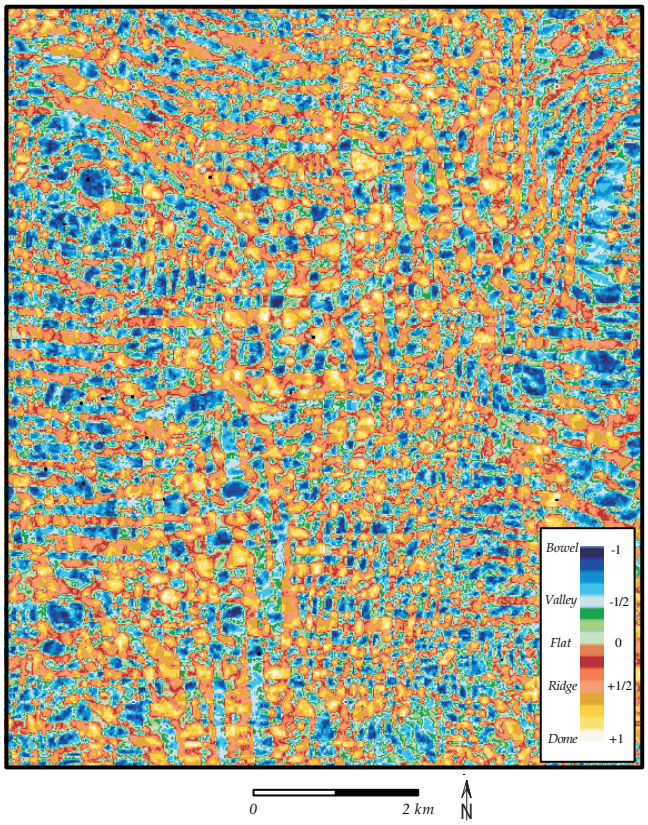

Fig.22 *Shape Index* S_i.

Fig.23 *Dip curvature,* K_d.

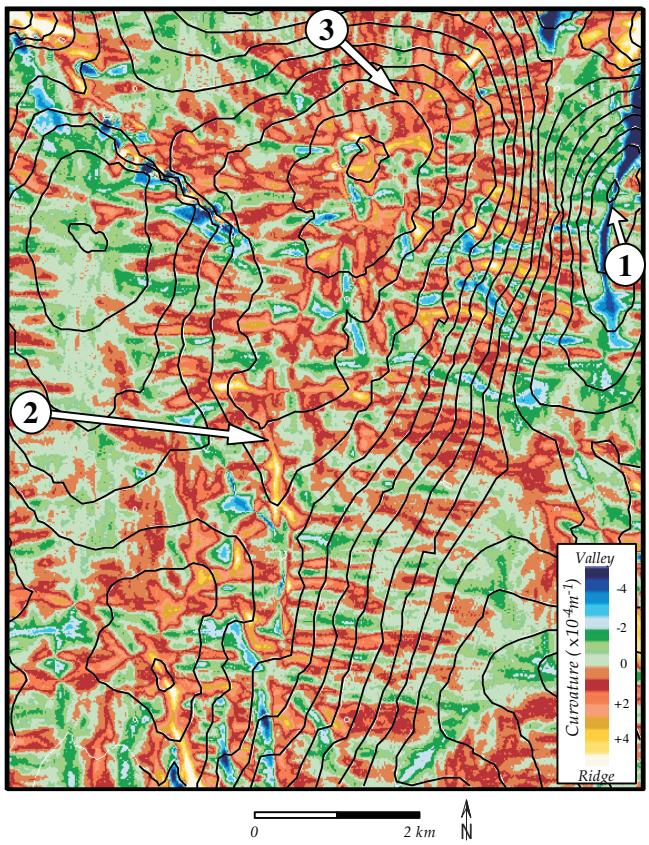

Fig.24 *Strike curvature,*K_S with time contours overlaid. See text for details.

depositional features such as dunes, clinoforms and offshore tidal bars. The seismic data, from which the surface has been mapped, can also contain false curvature features e.g. velocity pull-ups and push-downs and apparent faulting created by noise contamination (Hesthammer 1999).

It is therefore important to calibrate the curvature attribute to known fracture intensities. This calibration requires comparison of the fracture data to a suite of curvature attributes. This suite is derived using different aperture widths, in order to establish the scale or wavelength at which the extracted curvature correlates best to the fracture data. The effective aperture can be varied by a combination of smoothing and decimation (See discussion on scale of observation). Faults are also stress relief features and as discussed above, these can contaminate the local curvature values. It may therefore be appropriate to remove the effects of the faults on the mapped surface before a calibration is attempted.

Orientation of minimum and maximum curvature, $O_{\min}$ **and** $O_{\max}$

The azimuthal orientation of *minimum curvature* and *maximum curvature* can be extracted and are called the *principal directions*. The definition of the *orientation of minimum curvature,* $O_{\min}$ is illustrated in Fig.4. An example of the *orientation of maximum curvature,* $O_{\max}$ is displayed in Fig.21. Note that these two orientations will always be 90° apart. Examination of Euler's curvature formula (Eqn.4) displayed in Fig.5 shows that this orientation only needs to be defined between 0° and 180°. If the curvature can be calibrated to the stress state of a surface, then this type of attribute can help define the orientation of the minimum and maximum stress. These stress states may for example be related to an open fracture system. Once a successful calibration is achieved, then maps of O_{min} and O_{max} can be used to help optimise the trajectory of a horizontal well, maximising the intersection with the open fracture system. As with the *azimuth* attribute, O_{min} and O_{max} are very sensitive to noise and other rapid fluctuations in the surface. Consequently, the surface may require additional filtering and smoothing in order to obtain a more stable result. Other methods of display for this type of attribute are also used e.g. the orientation of curvature at each grid node is represented by a line rather than a colour code (See Figures 12 and 13 in Lisle 1995).

Shape Index, S_i

Fig.6 illustrates how combining curvature attributes allows the local surface shape to be defined. This type of approach results in only a qualitative description of shape. The *maximum* and *minimum curvatures* can be combined using Eqn.22 (Koenderink & van Doorn 1992) to derive the *shape index*:

$$S_i = \frac{2}{\pi} * \tan^{-1}\left[\frac{(K_{\min} + K_{\max})}{(K_{\max} - K_{\min})}\right] \qquad (25)$$

This allows an elegant quantitative definition of shape, which describes the local morphology of a surface independent of scale. In other words, a bowl is a bowl whether it is the size of a soup bowl or a radio telescope. The attribute is colour coded to reflect the local morphology in terms of bowl, valley, flat, ridge and dome shapes and this is illustrated in Fig.22. Because this attribute is not affected by the absolute magnitude of curvature (with the exception of planar surfaces), very subtle fault and map lineaments can be enhanced, as well as other surface patterns.

Dip Curvature, K_d

Extracting the curvature in the direction of maximum dip defines the *dip curvature* (Eqn.23), which is illustrated in Fig.23. This curvature is a measure of the rate of change of dip in the maximum dip direction and is called the *profile curvature* in Terrain Analysis (Wood 1996). Both the magnitude and direction of faults is preserved with this attribute. The black/white colour table used in creates an image similar to a shaded relief type of horizon display. This curvature method tends to exaggerate any local relief contained within the surface and can be used to enhance differentially compacted features, such as channelised sand bodies and debris flows.

$$K_s = \frac{2\left(ae^2 - cde + bd^2\right)}{\left(d^2 + e^2\right)\left(1 + d^2 + e^2\right)^{1/2}} \qquad (23)$$

Strike Curvature, K_S

Extracting the curvature in a direction which is at right angles to the *dip curvature* i.e. along strike, gives us the *strike curvature* (Eqn.24). This is sometimes referred to as the *tangential curvature* (Mitasova & Hofiefka 1993) and describes the tangential morphology or shape of the surface.

$$K_s = \frac{2\left(ae^2 - cde + bd^2\right)}{\left(d^2 + e^2\right)\left(1 + d^2 + e^2\right)^{1/2}} \qquad (24)$$

It separates the surface into areas of valley shapes (blue/green colours) and ridge shapes (yellow/red colours), as indicated by 1) and 2) respectively in Fig.24. This type of attribute is used extensively in Terrain Analysis, particularly in the area of gravity-driven processes, such as soil erosion and drainage (Moore *et al.* 1993). Turning this upside-down, this method can be used to examine the influence a top surface map may have on buoyancy-driven processes, such as hydrocarbon migration and production drainage efficiency. It is not just the local morphology that is important, but how that morphology is connected. For example, note how the ridges are connected on the flanks of the large anticline, which creates a dendritic drainage pattern indicated by 3) in Fig.24. In defining this connectivity, this type of display can help in understanding regional hydrocarbon migration pathways, together with areas of possible bypass. The magnitude of the *dip curvature* is also important, as higher values imply better developed local ridges or valleys. Note that computing the average of the *strike curvature* and *dip curvature* will result in the *mean curvature* (Eqn.3), as they are orthogonal curvatures.

Contour Curvature, K_C

Although *contour curvature* (sometimes referred to as *plan curvature*) is not a *normal curvature*, it is often used in other disciplines. Examination of Eqn.25 (Mitasova & Hofiefka 1993) shows that is very similar to the *strike curvature* (Eqn.24) and effectively represents the curvature of the map contours associated with the surface, created by cutting horizontally through the surface. Although this attribute is visually similar to the *strike curvature*, the *contour curvature* values are not well constrained and consequently very large values occur at the culmination of anticlines, synclines, ridges and valleys.

$$K_c = \frac{2\left(ae^2 - cde + bd^2\right)}{\left(1 + d^2 + e^2\right)^{3/2}} \qquad (25)$$

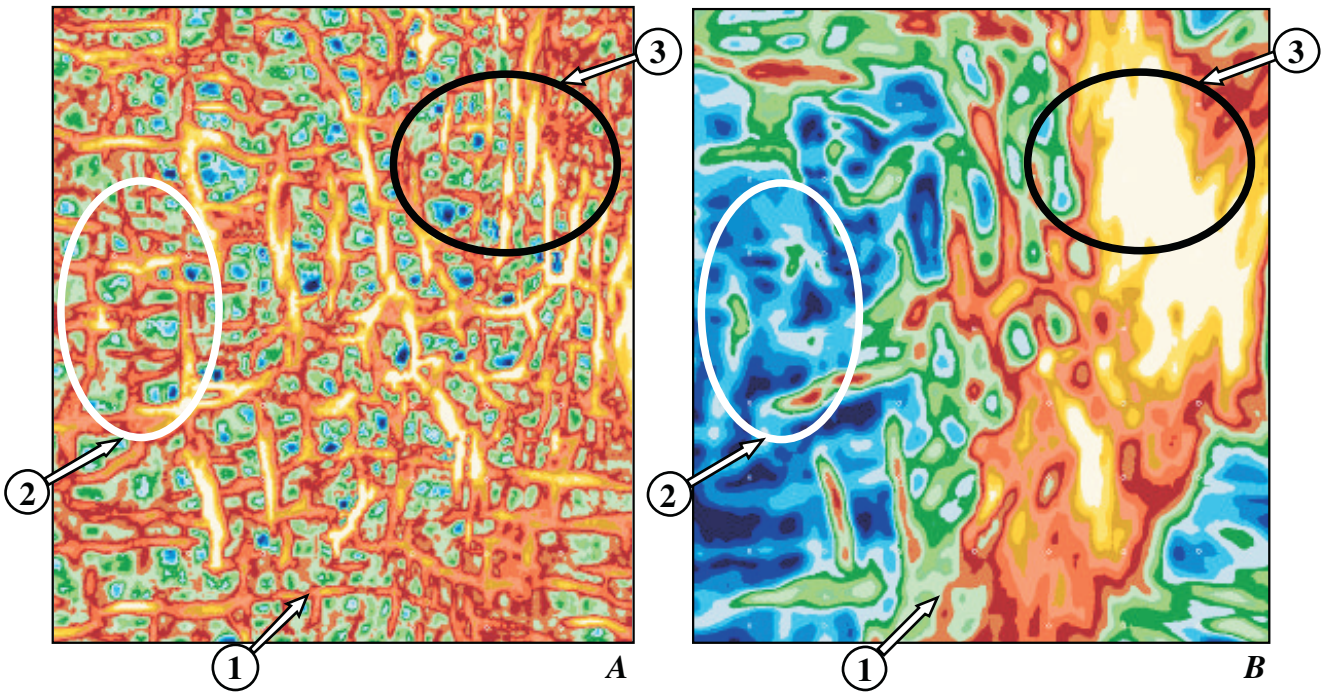

Fig.25 Comparison of attributes. A and B are enlarged versions of Fig.17 and Fig.10 respectively. 1) Minor east-west oriented lineaments are more clearly defined on the curvature attribute. 2) Comparing the data within the white rings show that curvature reveals many more surface lineaments. 3) Illustrates the problem of dip saturation. The north-south oriented lineaments, clearly observed within the black ring on the curvature attribute, are totally obscured by the high local background dip present on the dip angle.

Curvedness, K_n

The *curvedness* attribute, defined by Eqn.26, describes the magnitude of curvature of a surface independent of its shape (Koenderink & van Doorn 1992).

$$K_n = \sqrt{\left(\frac{K_{max}^{\ 2} + K_{min}^{\ 2}}{2}\right)} \qquad (26)$$

Describing the curvature in this absolute sense gives a general measure of the amount of total curvature present within the surface.

Comparison with existing attributes

Curvature attributes can reveal a lot of additional information relating to faults, lineaments and local shape contained within a surface. The *edge*, *dip* and *azimuth* attributes, as well as other methods such as the coherency cube (Bahorich & Farmer 1995), are the most common techniques used by seismic interpreters to identify faults. However, the first derivative methods only delineate lineaments and cannot differentiate between asymmetric features, such as faults or rapid dip changes, and symmetric features, such as ridges or valleys. This is because these attributes contain no shape information. Consequently, it is difficult to make direct comparisons of these techniques to many of the curvature attributes, with the exception of the *most negative* and *most positive curvatures*. Fig.25 is a comparison between the *dip angle* attribute and the *most negative curvature*. This figure indicates that curvature is better at detecting surface lineaments and does not suffer from the problem of *dip saturation*. This effect often occurs in areas of higher dip, where the high background dip values obscure the smaller faults and lineaments which may be present within the surface. Curvature is surface orientation independent, which means that provided the surface is adequately sampled (unaliased), then the curvature value remains unchanged, even if the surface is rotated or tilted. This is not the case with the first derivative methods, where tilting or rotation clearly changes the attribute values. Consequently, the ability of the first derivative methods to adequately detect faults depends on the specific geometry of the fault and these limitations are summarised in Table 1. This table suggests that *dip* and *azimuth* attributes, even when used in combination, will not necessarily detect all fault geometries. On the other hand, curvature copes well with all these cases.

Illumination or shaded relief attributes also appear to be a good delimiter of faults and lineaments (Brown 1996). Unfortunately these methods are sensitive to the position of the sun source and require a certain degree of user interaction to optimise the display. Situations where faults and lineaments occur along many different orientations often require multiple displays with differing sun source locations. Curvature, being surface orientation independent, allows almost all of the information to be captured in only one display.

	Fault Type	Dip/Edge	Azimuth	Curvature
Flat		*Good*	*Variable*	*Good*
Increasing dip		*Good*	*None*	*Good*
		Good	*Good*	*Good*
		Poor	*None*	*Good*
Steep		*Poor*	*Good*	*Good*

Table 1. Summary of fault delineation ability of attributes. With the exception of curvature, the ability of an attribute to detect faults depends on the geometry of the fault.

Conclusion

Curvature attributes potentially offer a powerful insight into mapped surfaces. It is surprising that the oil industry has been slow to utilise curvature attributes and this may partly stem from our rather limited exposure to disciplines other than our own. It is interesting to note that the *dip* and *azimuth* attributes, which appeared just over ten years ago (Dalley *et al.* 1989), were already well-established in other disciplines at that time e.g. Terrain Analysis (Young 1979). The advent of the internet will hopefully change this for good, as it probably offers the best vehicle for scientific ideas and techniques to be readily exchanged between a wide spectrum of disciplines.

Curvature is a second derivative based method and consequently is sensitive to any noise contamination which may be present within the surface. This often necessitates the surface to be pre-processed using some form of spatial filter, which can be iterated. The scale of investigation is another important consideration in the computation of curvature. The scale is controlled by the aperture and sampling interval sizes. These are selected based on values appropriate for the scale of the problem being investigated i.e. larger apertures for regional effects or smaller apertures for local surface detail.

The curvature attributes presented in this paper, although they represent only a small subset, have been selected based on their applicability to seismic interpretation. Each of the individual curvature attributes all give a slightly different insight into the mapped surface. For example, *maximum curvature* offers a number of additional benefits over the first derivative based methods (*dip, edge* and *azimuth*), which are commonly used in fault delineation. Curvature contains the added dimension of shape, allowing faults, fault orientations and fault geometries to be delimited, as well as discriminating faults from other linear surface features. Comparisons between the *dip angle* and *most negative curvature* indicate that curvature can delineate many more surface lineaments, without suffering from the problem of *dip saturation*. Curvature avoids this problem because it is surface orientation independent. *Strike curvature* describes the local surface morphology in terms of ridges and valleys, which can be used to visualise drainage patterns, with potential applications in understanding well drainage efficiency and in the mapping of hydrocarbon migration pathways. *Shape index* allows a quantitative description of local surface shape, with a more qualitative description being derived from a combination of *mean curvature* and *Gaussian curvature*. With careful calibration to well data, curvature can be used to understand the stress regime of a surface and help predict the distribution of fracture densities as well as the orientation of the principal stress directions.

Curvature can also be computed in the volume sense, although this particular aspect is beyond the scope of this paper. In calculating this type of volume attribute, the success of the algorithm depends mainly on the ability to define an accurate local surface for each sample within the volume. The curvature of this local surface can then be easily computed using an approach similar to those presented in this paper.

It must be stressed that no surface attribute, including curvature, should be used in isolation. All map attributes should be interpreted with reference to the original seismic from which the surface was created. In general, a large part of any gridded surface does not usually represent a continuous manual interpretation, but data created by an horizon autotracker. The process of checking the attribute against the original seismic data is often the only possibility to check both the input mapped surface and the attribute results. This type of quality control often requires that additional manual interpretation be carried out, but results in a better understanding of the data problems (noise), as well an improved final attribute.

References

Bahorich, M. and Farmer, S. [1995] The coherence cube. *The Leading Edge*, **14**, No. 10, 1053-1058

Brown, A. [1996]. Interpretation of three-dimensional seismic data. 4th Edition. *AAPG Memoir 42*.

Dalley, R.M., Gevers, E.C.A., Stampfli, G.M., Davies, D.J., Gastaldi, C.N., Ruijtenberg, P.A. and Vermeer, G.J.O. [1989] Dip and azimuth displays for 3D seismic interpretation. *First Break*, **7**, No. 3, 86-95

Daniel, M. and Barsky, B. [1997] Discrete Gaussian curvature for analysis of a B-spline modeled cornea", *SIAM Conference on Geometric Design*, Nashville, Nov. 3-6, 1997.

Evans, I.S. [1979] An integrated system of terrain analysis and slope mapping. *Final report on grant DA-ERO-591-73-G0040*, University of Durham, England.

Flynn, P.J. and Jain, K.J. [1989] On reliable curvature estimation. *IEEE Conference on Computer Vision and Pattern Recognition*, San Diego, 110-116

Gallagher, N.C. and Wise, G.L. [1981] A theoretical analysis of the properties of median filters. *IEEE Transactions on Acoustics, Speech, and Signal Processing*, **ASSP-29(6)**, 1136-1141.

Gauss, C.F. [1827] Disquisitones generales circa superficies curvas (General investigation into curved surfaces).

Hesthammer, J. [1999] Improving seismic data for detailed structural interpretation. *The Leading Edge,* **18**, No, 2, 226-247.

Joshi, S. C., Wang, J., Miller, M. I., Van Essen, D. C., and Grenander, U. [1995] On the differential geometry of the cortical surface. *Proceedings of the SPIE's 1995 International Symposium on Optical Science, Engineering, and Instrumentation. Vision Geometry IV*, **2573**, 304-311.

Koenderink, J.J. and van Doorn, A. J. [1992] Surface shape and curvature scales. *Image and Vision Computing*, **10(8)**, 557-565.

Lisle, R.J. [1994] Detection of zones of abnormal strains in structures using Gaussian curvature analysis. *AAPG Bulletin*, **78(12)**, 1811-1819.

Lisle, R.J. [1995] The Mohr circle for curvature and its application to fold description. *Journal of Structural Geology*, **17(5)**, 739-750.

Marcus, H. [1932] Die Theorie elastischer Gewebe. 2nd edition, Berlin.

Murray, G. H. [1968] Quantitative fracture study – Spanish Pool, McKenzie County, North Dakota. *The American Association of Petroleum Geologists Bulletin*, **52(1)**, 57-65.

Mitasova, H. and Hofierka, J. [1993] Interpolation by regularised spline with tension : II. Application to terrain modeling and surface geometry analysis. *Mathematical Geology*, **25**, 657-669.

Moore, I.D., Gessler, P.E., Nielsen, G.A., and Petersen, G.A. [1993] Soil attribute prediction using Terrain Analysis. *Soil Sci. Soc. Am. J.*, **57**, 443-452.

Nielsen, N.J. [1920] Bestemmelse af Spændinger i Plader. Copenhagen.

Peet, F.G. and Sahota, T.S. [1985] Surface curvature as a measure of image texture. *IEEE Transactions on Pattern Analysis and Machine Intelligence*, **PAM1-7(6)**, 734-738.

Price, N.J. and Cosgrove, J.W. [1990] Analysis of geological structures. Cambridge University Press, Cambridge.

Rektorys, K. [1969] Survey of applicable mathematics. MIT Press, Cambridge, MA ; Iliffe Books Ltd. Chapter 9. Differential Geometry, 298-373.

Stewart, R. and Podolski, S.A. [1998] Curvature analysis of gridded surfaces. In: Coward, M.P., Daltaban, T.S. and Johnson, H. (eds*) Structural Geology in Reservoir Characterization*. Geological Society, London, Special Publications, **127**, 133-147.

Thomas, G.B. [1972] Calculus and analytical geometry. Fourth edition. Addison-Wesley Publishing Company.

Timoshenko, S. and Woinowsky-Krieger, S. [1959] Theory of plates and shells. 2nd Edition. McGraw-Hill.ISBN 0-07-085820-9

Wen, R. and Townsend, C. [1997] Seismic attributes for mapping small scale faults in reservoirs. *59th EAEG conference in Geneva*. Presentation C010.

Wood, J.D. [1996] The geomorphological characterisation of Digital Elevation Models, *PhD Thesis*, University of Leicester.

Young, M. [1978] Statistical characterisation of attribute matrices by computer. *The fifth progress report on Contract DA-ERO-591-73-G0040*. U.S. Army European Research Office, London. Report 5, 1-16